Iterative Halftoning Using Spectral Constraints

Thomas Scheermesser and Olof Bryngdahl
University of Essen, Physics Department
45117 Essen, Germany

Abstract

Iterative halftoning algorithms offer great flexibility in adapting the halftoning process to specific demands. Constraints defined in the Fourier domain can be used to synthesize images with a wide variety of characteristics. Using such constraints, the halftoning process and the resulting image can be adapted to the characteristics of a processing system or the graytone original. Moreover, a control of image texture can be realized and combined with other constraints.

Introduction

In recent years, digital halftoning techniques have gained constantly increasing interest because of the widespread use of binary output devices. The desire to display images with the highest achievable quality within the limited capabilities of such devices has led to different types of algorithms, such as carrier procedures,[1] error diffusion,[2] and iterative algorithms,[3] all of which have different properties. In general, the progress in research has resulted in increased flexibility in adapting the process of binarization to specific situations, device characteristics, image properties, applications, etc.

Iterative algorithms offer by far the most flexibility in synthesizing the desired image. Nearly all mathematically consistent constraints can be realized. Various types of iterative algorithms exist, e.g., direct binary search, simulated annealing,[4] and Hopfield neural networks,[5] all of which can and have been applied to halftoning. The most attractive one seems to be the iterative Fourier transform algorithm (IFTA),[3] due to its relatively fast convergence and the physical importance of the Fourier transform. There are various types of constraints that can be formulated in the spectral domain, based on the physical situation for which the image is intended or on properties of the image itself. In this paper, we present an overview of possible spectral constraints and their realization and limitations, along with examples to illustrate the effects. Among the constraints presented are well-known procedures, such as lowpass[3,6] or phase control,[7] as well as new ideas, e.g., control of the noise remaining inside a low-pass region or texture control.

2 The Physical Situation

Before we discuss the various spectral constraints, the physical situation and the general structure of the algorithm are outlined. Consider a graytone original:

$$f(m,n) \in [0,1], \qquad m,n \in \{1, \ldots, N\}, \tag{1}$$

i.e., a real-valued, sampled, two-dimensional intensity distribution. The graytone original $f(m,n)$ is transformed by the halftoning algorithm into the image

$$g(m,n) \in (v_1, \ldots, v_z), \tag{2}$$

quantized to z levels (Fig. 1). In this paper, binary images are considered ($z = 2$, $v_1 = 0$, $v_2 = 1$), but almost all of the argumentation also applies to an arbitrary number of quantization levels. The halftoning algorithm is represented by the operator $\mathcal{Q}$, such that

$$g(m,n) = \mathcal{Q} f(m,n). \tag{3}$$

After the image is displayed on the output device, it is fed into a processing system T, resulting in a modified distribution $s(x,y)$, with $x,y \in \mathbb{R}$. Characteristics of the output device, such as dot overlap or dot size and positioning errors, are neglected here for simplicity. Some of these effects can be considered, to a sufficient degree, by a precompensation of the graytone image, while others would require a modification of the halftoning algorithm based on knowledge about the characteristics of the specific device.[8] Therefore, we have

$$s(x,y) = T g(m,n). \tag{4}$$

Note that $s(x,y)$ is not necessarily a sampled distribution. The system T can represent any processing system and the knowledge about its characteristics may be used to state constraints of the binary image.

For example, if the image is viewed by a human observer, T could stand for the imaging part of the visual system and $s(x,y)$ for the retinal image. The linear systems theory describes such a system to a good approximation and leads to specific constraints of the Fourier spectrum of the binary image (Sec. 4). Knowledge about the processing of $s(x,y)$ by the retina and the cortex may be incorporated in T and result in modified spectral constraints.

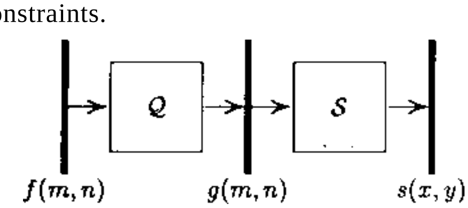

Figure 1. Schematic diagram of the physical situation: The graytone original $f(m,n)$ is halftoned by $\mathcal{Q}$ and fed into the processing system T, resulting in the distribution $s(x,y)$.

3 The Iterative Halftoning Algorithm

Often the required characteristics can be stated adequately in the spectral domain and the IFTA is well suited to implement a binarization. It is based on a successive Fourier and inverse Fourier transform, where operations on the current image are performed in the spatial and frequency domains. After a sufficient number of iterations, say, N, this leads to a binary image with the desired spectral constraints:

$$\begin{aligned} g(m,n) &= Qf(m,n), \\ &= [BF^{-1}PF]^N \hat{B} f(m,n). \end{aligned} \tag{5}$$

Figure 2 illustrates the structure of the algorithm. The terms F and F^{-1} indicate the Fourier transform and its inverse, and P performs the operation in the Fourier domain, which ensures the spectral characteristics of the resulting image. The specific structure of P depends on the actual constraints and is shown in later sections.

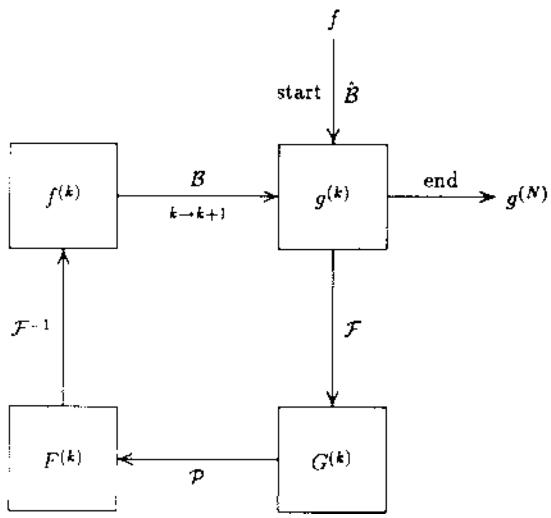

Figure 2. Schematic diagram of the iterative Fourier transform algorithm.

The operator B acts in the spatial domain and ensures that the resulting image is binary. The choice of B is crucial for the proper convergence of the algorithm. However, there exist different possibilities.[3,6] For the examples in this paper, B was chosen for

$$\begin{aligned} g^{(k+1)}(m,n) &= Bf^{(k)}(m,n) \\ &= \begin{cases} 1 & \text{if } f^{(k)}(m,n) \geq 1-\Delta \\ 0 & \text{if } f^{(k)}(m,n) \leq \Delta \\ \text{step}[f^{(k)}(m,n) - z^k(m,n)] & \text{otherwise} \end{cases}, \end{aligned} \tag{6}$$

where $z^k(m,n) \in [0,1]$ is a pseudorandom number, $\Delta \in [0,1/2]$ is a free parameter, and

$$\text{step}(x) = \begin{cases} 1 & \text{if } x \geq 0 \\ 0 & \text{if } x < 0 \end{cases}. \tag{7}$$

The choice of Δ is important to avoid stagnation and ensure an optimal result of the algorithm, but it is not discussed in greater detail here. The operator $\hat{B}$ generates a start distribution from the original graytone image and is often, but not necessarily, identical with B. The algorithm terminates after N cycles, either when a predefined quality criterion is reached or after a fixed number of cycles. Satisfactory results are typically achieved within about 30 to 50 cycles.

Another point that should be considered is that the displayed binary image is not repeated and thus possesses a continuous spectrum, contrary to its mathematical representation implied by the discrete Fourier transform, which is periodically repeated and discrete in both the spatial and the Fourier domain. When the quantization is carried out by a digital device using the discrete Fourier transform, the noise between the sampling points remains uncontrolled and is present in the final image. To avoid this, the sampling frequency in the Fourier domain should at least be doubled, which is easily done by modifying the operator B in such a way that the image is placed centrally in a black field twice as large as the graytone original.[9]

4 Constraints Based on the Processing System

Consider again the situation shown in Fig. 1. The binary image is fed into a processing system T. If this system is linear, its characteristics are completely described by its transfer function $H(\mu,v)$, and the effect on $g(m,n)$ can easily be stated in the Fourier domain:

$$S(\mu,v) = H(\mu,v)G(\mu,v), \tag{8}$$

where $S(\mu,v)$ and $G(\mu,v)$ are the Fourier transforms of $s(m,n)$ and $g(m,n)$, respectively.

It is often desirable for the system to be unable to distinguish between the original and the binary image, so that

$$H(\mu,v)G(\mu,v) = H(\mu,v)F(\mu,v), \tag{9}$$

where $F(\mu,v)$ is the Fourier transform of $f(m,n)$. Because the shape of $H(\mu,v)$ is given, this leads directly to the spectral constraint

$$G(\mu,v) = F(\mu,v) \qquad \text{if } H \neq 0. \tag{10}$$

The support region of $H(\mu,v)$ must be sufficiently small, because the spectra of the two images are necessarily different [if $f(m,n)$ is not itself binary] and thus $G(\mu,v) = F(\mu,v)$ cannot be true in the whole Fourier domain. In other words, there must be enough room for the introduction of the quantization noise spectrum. A description of the limitations for the size of the support region of $H(\mu,v)$ is given in Sec. 7.

4.1 Lowpass Control

The concept of an iterative control of a lowpass region was proposed by Broja, Wyrowski, and Bryngdahl[3] to adapt the quantization noise spectrum to the characteristics of the human visual system.[10] The imaging part of the eye can be regarded to a good approximation as an incoherent imaging system with a circular exit pupil. The transfer function of such a system vanishes outside a circular region Ω_1 with radius μ_c, which is the cutoff frequency (Fig. 3). If all of the quantization noise spectrum were removed from Ω_1, the observer would not be able to distinguish between the original and the binary image. Such a procedure can be realized with *P* by replacing the spectrum inside Ω_1 with the original spectrum, i.e.,

$$F^{(k)}(\mu,v) = PG^{(k)}(\mu,v) = \begin{cases} F(\mu,v) & \text{if } (\mu,v)\in\Omega_1 \\ G^{(k)}(\mu,v) & \text{otherwise} \end{cases}. \quad (11)$$

In general, some noise will remain in the control region, because the existence of a binary image with a lowpass region exactly identical with that of the graytone original is not ensured. The smaller the extent of Ω_1, the easier it is to remove most of the noise from it, but then the resolution of the output device must be accordingly higher than that of the eye or, for a fixed device resolution, the minimal viewing distance is larger. It is thus desirable to control a region as large as possible. In Fig. 4, an image halftoned in this way is shown along with its quantization noise spectrum. The extent of Ω_1 is approximately 29% of the spectrum. One can see clearly that most of the noise is removed from the lowpass region. The largest areas possible to control with this algorithm are around 33% of the spectrum. The actual value depends on the particular image.

4.2 Control of the Remaining Noise

The remaining noise has the tendency to concentrate around the dc peak, particularly for large control regions. This is the most unfavorable position, because $H(\mu,v)$ has its maximum there. This behavior can be easily understood as follows: The algorithm in its form described previously has the tendency to minimize the noise energy in the control region. A measure for the noise energy is

$$\sigma^2 = \frac{\sum_{(\mu,v)\in\Omega_1} \left|G(\mu,v) - F(\mu,v)\right|^2}{\sum_{(\mu,v)\in\Omega_1} 1}.$$

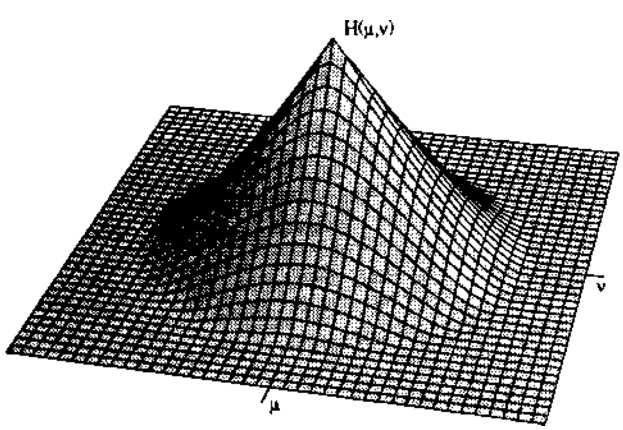

Figure 3. Transfer function of a diffraction-limited incoherent imaging system with a circular exit pupil.

If Ω_1 covers the whole spectrum, it follows from Parseval's theorem that the hardclip with a clipping level equal to one-half yields[11] an image with a minimum of σ^2. No other halftoning algorithm can produce a lower σ^2. Because the IFTA tends to minimize σ^2 in Ω_1, it will produce an image similar to the hardclip if Ω_1 encloses the whole spectrum. The distribution of the noise spectrum of a hardclip is oriented at the spectrum of the graytone original, and because this is concentrated around the dc peak for usual images, so is the noise spectrum. If the size of Ω_1 is increased from close to zero to an extent that covers the whole spectrum, consequentially more and more of the noise remaining inside Ω_1 will concentrate around the dc peak.

To avoid this behavior, we propose to modify *P* in a way that the remaining noise is shifted to the border of $H(\mu,v)$:

$$F^{(k)}(\mu,v) = P_\xi G^{(k)}(\mu,v) = F(\mu,v) + \xi(\mu,v)[G^{(k)}(\mu,v) - F(\mu,v)], \quad (13)$$

where $\xi(\mu,v)$ is a scalar function, which weights the noise inside Ω_1, with

$$\xi(\mu,v) = 1 \qquad \text{if } (\mu,v)\notin\Omega_1. \quad (14)$$

The smaller the integral over $\xi(\mu,v)$ is, the less noise is tolerated in each iteration cycle and the lower is the total noise energy remaining in Ω_1. Because the algorithm is forced to produce a different noise distribution than before, σ^2 is likely to increase. But because the noise may now be located near μ_c, where $H(\mu,v)$ is close to zero, the transmitted noise energy, i.e, the energy of the noise weighted with the transfer function, will probably be reduced.

The difficulty lies in minimizing the noise in Ω_1 and at the same time introducing the desired characteristic. To find an optimal compromise between a minimum of the total remaining noise energy inside Ω_1 and a minimum of noise around the dc peak, an appropriate $\xi(\mu,v)$ must be chosen. We have performed several experiments and found

$$\xi(\mu,v) = \begin{cases} \left[\dfrac{(\mu^2+v^2)^{1/2}}{\mu_c}\right]^{1.2} & \text{if } (\mu,v)\in\Omega_1 \\ 1 & \text{otherwise} \end{cases} \quad (15)$$

to be a good choice. In Fig. 5, an image halftoned in this way and its quantization noise spectrum are shown. Again, Ω_1 was chosen as approximately 29% of the spectrum. Compared with Fig. 4, the noise around the dc peak has almost completely vanished and the image has a noticeably finer texture.

As expected, the value of $\sigma^2 = 4.5$ for the image in Fig. 5 is higher than for the image in Fig. 4 ($\sigma^2 = 1.6$). If the noise spectrum is multiplied with the transfer function before σ^2 is computed, this yields $\sigma_H^2 = 5.3$ for the image in Fig. 5, compared to $\sigma_H^2 = 10.4$ for the image in Fig. 4. The distribution of the remaining noise is thus adapted to $H(\mu,v)$, and a smoother visual appearance of the binary image is achieved.

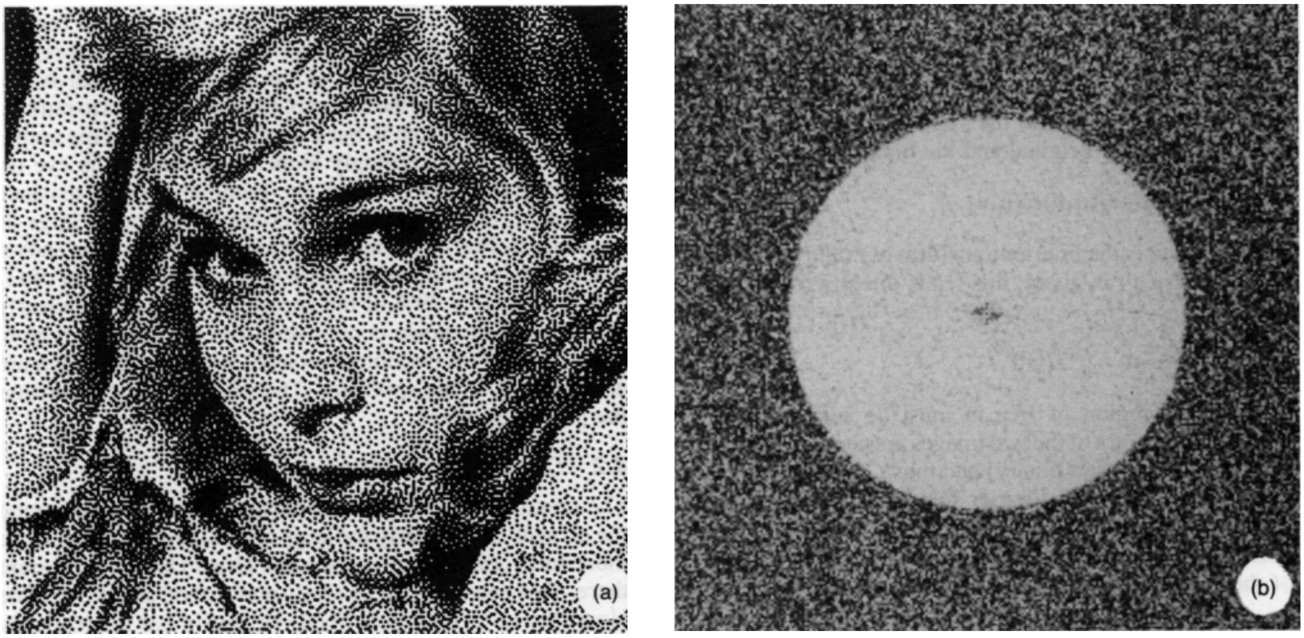

Figure 4. (a) Image halftoned by controlling a circular lowpass region Ω_1 of approximately 29% of the spectrum and (b) the quantization noise spectrum of part (a).

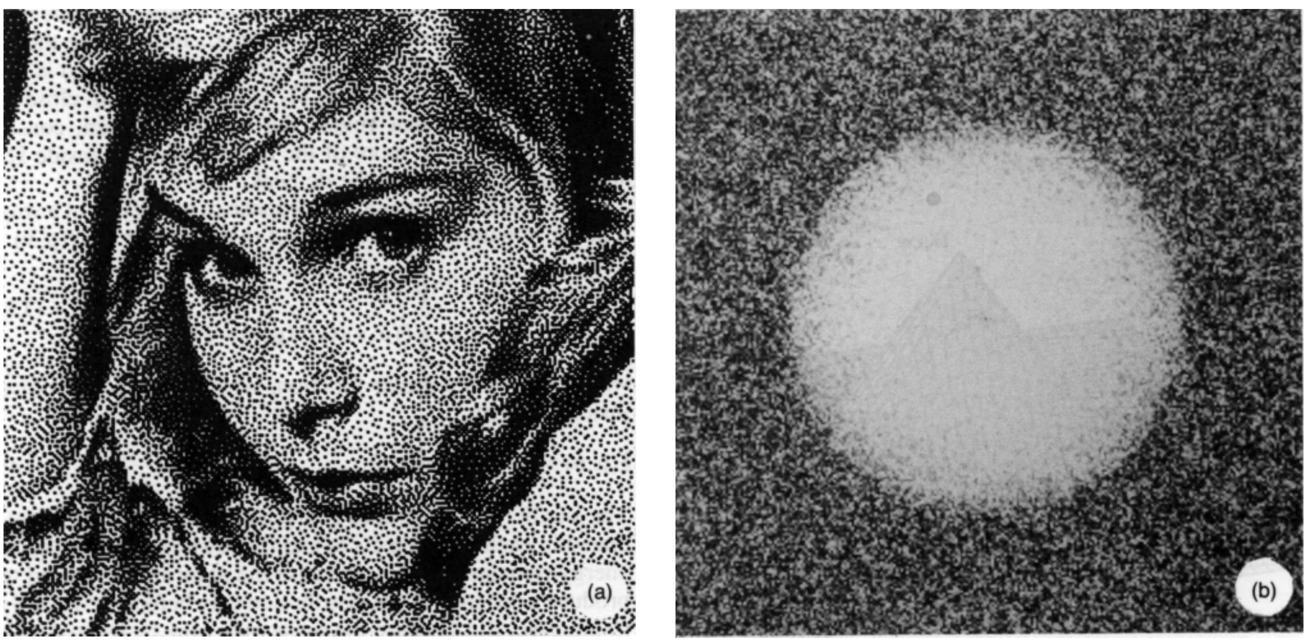

Figure 5. (a) Image halftoned by controlling a circular lowpass region Ω_1 of approximately 29% of the spectrum, with additional control of the structure of the noise remaining in Ω_1 and (b) quantization noise spectrum of part (a).

5 Constraints Based on Image Properties

To base the constraints of the noise spectrum on the processing system is a plausible approach. However, it makes sense only if enough information about the effect of the system on the image spectrum is available and its transfer function has an appropriate form. Otherwise, it is still useful to consider the processing system, but other approaches to shape the noise spectrum may also make sense. If all or most of the spectrum is transferred by $H(\mu,\nu)$, the general goal could be to conserve as much of the information as possible of the graytone original during the halftoning process. The problems are to identify the interesting parts of the information and to implement the binarization appropriately.

5.1 Phase Control

Much of the information of an image is contained in the phase of its Fourier spectrum, especially about edges and details.[12] A compromise between the introduction of noise and the preservation of the original spectrum is to adapt the phase of the spectrum of the binary image to

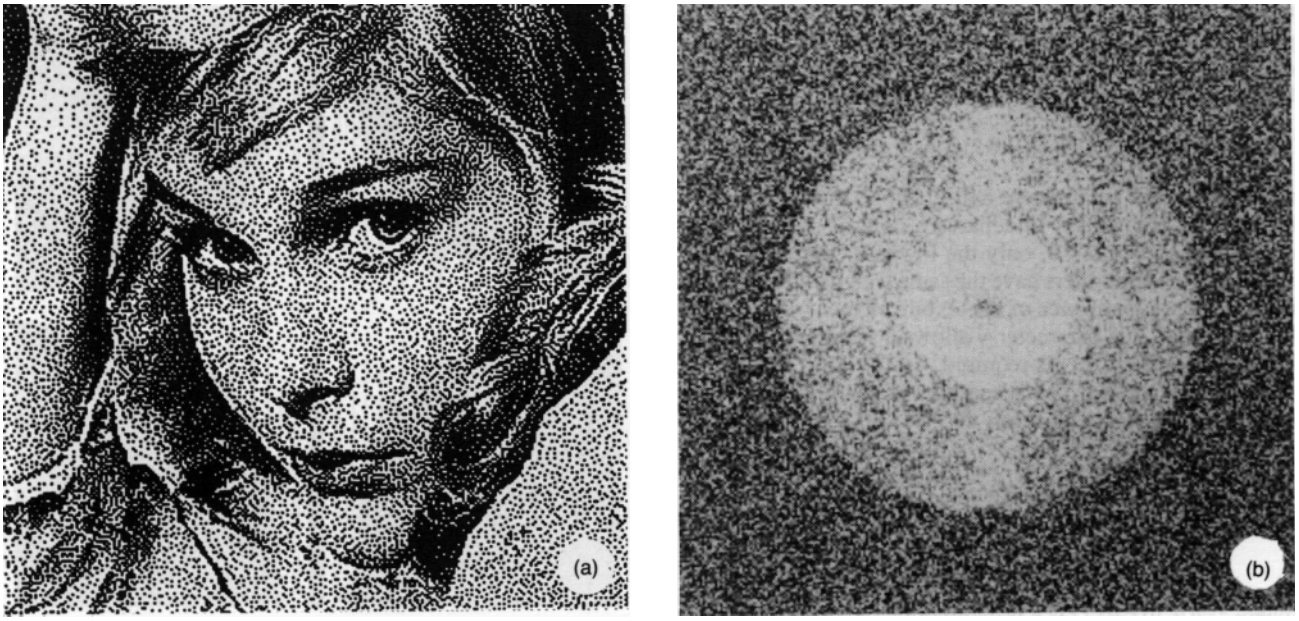

Figure 6. (a) Image halftoned by controlling a circular lowpass region of 5% in amplitude and phase, and a bandpass region of 20% in phase only, and (b) quantization noise spectrum of part (a).

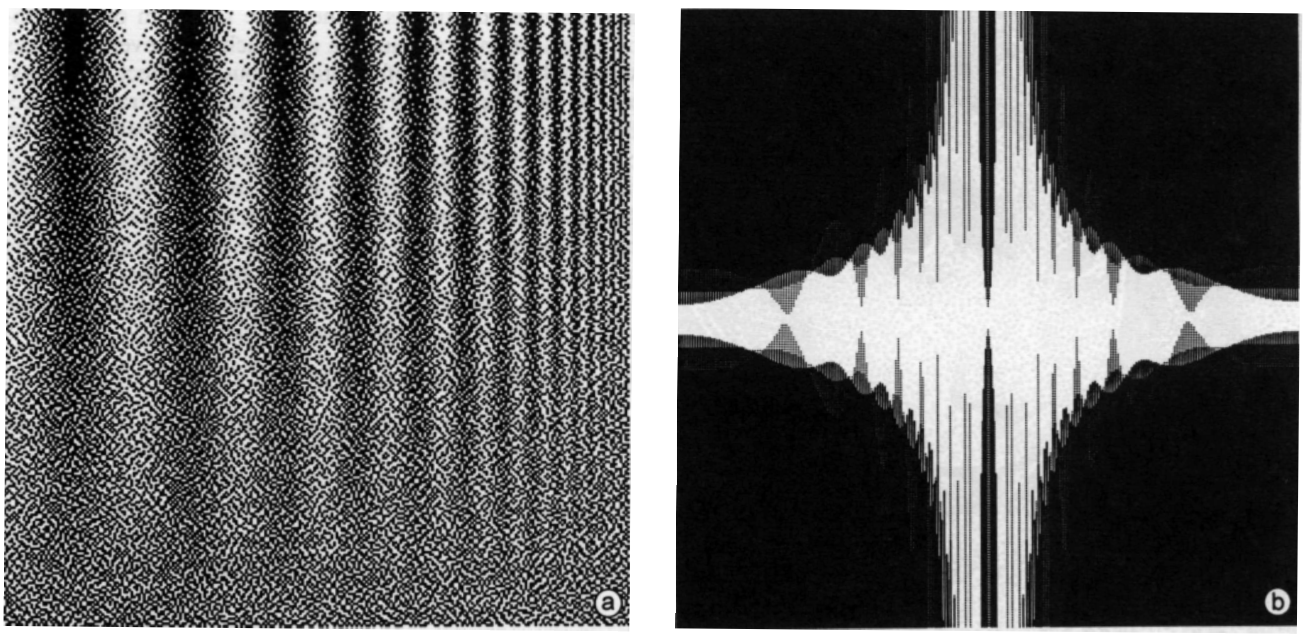

Figure 7. (a) Image halftoned with an adapted control area and (b) control area used for its synthesis.

that of the graytone original in some area Ω_2, but allow differences in the amplitude.[7] In this way, noise can be introduced in Ω_2 that is adapted to the phase of the graytone image spectrum. To implement this procedure, P is changed according to

$$F^{(k)}(\mu,v) = P_p G^{(k)}(\mu,v) = \begin{cases} F(\mu,v) & \text{if } (\mu,v)\in\Omega_1 \\ \left|G^{(k)}(\mu,v)\right| \exp\{i \arg[F(\mu,v)]\} & \text{if } (\mu,v)\in\Omega_2 \,. \\ G^{(k)}(\mu,v) & \text{otherwise} \end{cases} \quad (16)$$

Because the noise in Ω_2 is adapted to the phase of $F(\mu,v)$, this procedure results in an enhancement of details and edges. By varying the shape and size of Ω_1 and Ω_2, the amount of edge enhancement can be controlled.

Figure 6 shows an example that illustrates this procedure. The region Ω_1 consists of a circular lowpass covering 5% of the spectrum and Ω_2 consists of a ring-shaped bandpass with 20% extent. The edge enhancement is clearly visible in the image. In the noise spectrum, the control areas can be easily identified, because the amount of noise is reduced not only in Ω_1 but also in Ω_2. This is due to a coupling between the amplitude and phase in the spectrum of the binary image (Sec. 7). If the phase is controlled in a certain region, only a limited amount of noise can be introduced in the amplitude.[13]

5.2 Adaptation of the Control Areas

Another possibility to incorporate the image structure in the halftoning process is to modify the shape of the control areas. The parts of the spectrum are controlled that contain the information that should be transferred to the binary image, while in the remaining regions the quantization noise spectrum can be introduced.[9] A useful criterion of significance is the amplitude of the spectrum of the graytone original, $|F(\mu,v)|$. The control area may be defined via a threshold t_A,

$$\Omega_1 = [(\mu,v)||F(\mu,v) \geq t_A]. \tag{17}$$

Similarly, if the absence of specific spatial frequencies is relevant, a threshold t'_A can be introduced instead of or in addition to t_A, to control the spectrum where $|F(\mu,v)| < t'_A$.

Especially for images with an unusual distribution of their frequency content, this procedure may be advantageous. In Fig. 7 such an image is shown, along with the control area that was used for the binarization. The original image contains high frequencies in the horizontal and vertical direction but not along the diagonals. The spectrum is controlled according to these characteristics and the algorithm conserves the high-frequency content contrary to a lowpass control. The isolated points belonging to Ω_1 do not appear if the spectra are not oversampled. Oversampling can have a great effect on the shape of Ω_1 if defined according to Eq. (17). Of course, an additional threshold can be introduced to define a phase-control area, similar to that described in the previous section.

6 Control of Image Textures

The local arrangement of pixels, the image texture, is an important parameter. The visual system is very sensitive to specific patterns[14] and can easily detect a change in texture as a false contour. Also, for output devices, the texture often is of importance. For example, if the dots overlap, different orientations of a fixed number of pixels may yield different average gray values.

By modifying the operation in the image spectrum during the iteration, as proposed in this section, it is possible to influence the image texture. To do this, it is helpful to use the concept of texture elements, consisting of a few pixels arranged in a specific way. It is possible to enhance (or suppress) a specific texture characterized by a texture element $t(m,n)$ by modulating the noise according to its Fourier transform $T(\mu,v)$, i.e, the texture filter.[15,16] To achieve visually pleasing results, it is useful to combine this with a lowpass control. This is possible by combining $T(\mu,v)$ with a highpass filter $D(\mu,v)$, so that a modified texture filter

$$T'(\mu,v) = \gamma D(\mu,v)[(1-\alpha)+ \alpha T(\mu,v)] \tag{18}$$

is achieved. The parameter $\alpha \in [0,1]$ allows a weighted combination of both filters to achieve a control of the texture enhancement. For $\alpha = 0$, only the lowpass control remains, and for $\alpha = 1$, both filters have the same weight, which results in a strong predominance of the texture element $t(m,n)$ in the binary image. The parameter γ allows a scaling of the filter, because $T'(\mu,v) \in [0,1]$ is required.

A modification of P is necessary to shape the noise according to $T'(\mu,v)$. This leads to

$$\begin{aligned} F^{(k)}(\mu,v) &= P_r G^{(k)}(\mu,v) \\ &= \begin{cases} F(\mu,v) & \text{if } z^{(k)}(\mu,v) \leq 1 - T'(\mu,v) \\ G^{(k)}(\mu,v) & \text{otherwise} \end{cases}, \end{aligned} \tag{19}$$

where $z^{(k)}(\mu,v) \in [0,1]$ is a pseudorandom number. This procedure results in a noise distribution, which is globally modulated according to $T'(\mu,v)$. In Fig. 8, two examples for such filters and the resulting binary images are given. The texture element consists of two pixels, which are separated by two units in the horizontal and one in the vertical direction. To achieve an additional lowpass control, the resulting filter $T(\mu,v)$ was combined with another filter, which is obtained by the Floyd-Steinberg error diffusion algorithm and can be stated analytically.[17] A value of 1 was chosen for or in Fig. 8(a) and $\alpha = 0.25$ in Fig. 8(b). The texture element is clearly predominant in both images, especially in Fig. 8(a). Due to the simultaneous lowpass control, a good graytone rendition is also achieved.

7 Limitations of Spectral Constraints

As we have mentioned a few times in the prior description of different spectral constraints, there are limitations to which constraints can be realized. These limitations result from different mechanisms present during the binarization process.[13]

If oversampled spectra are used, the values in the spectrum are coupled by a system of N^2 linear equations. This coupling results directly from the sampling theorem. Let ω_i denote the number of sampling points in Ω_i, with $i \in \{1,2,3\}$. Then $2\omega_1 + \omega_2$ real values are predetermined by the constraints (amplitude and phase in Ω_1 and phase in Ω_2), and the system of equations has a unique solution if $\omega_1 \geq \omega_3$. This solution is nothing but the spectrum of the graytone original, which means that it is impossible to introduce quantization noise without violating the constraints. Consequently, to have enough freedom for the introduction of noise, it is necessary that

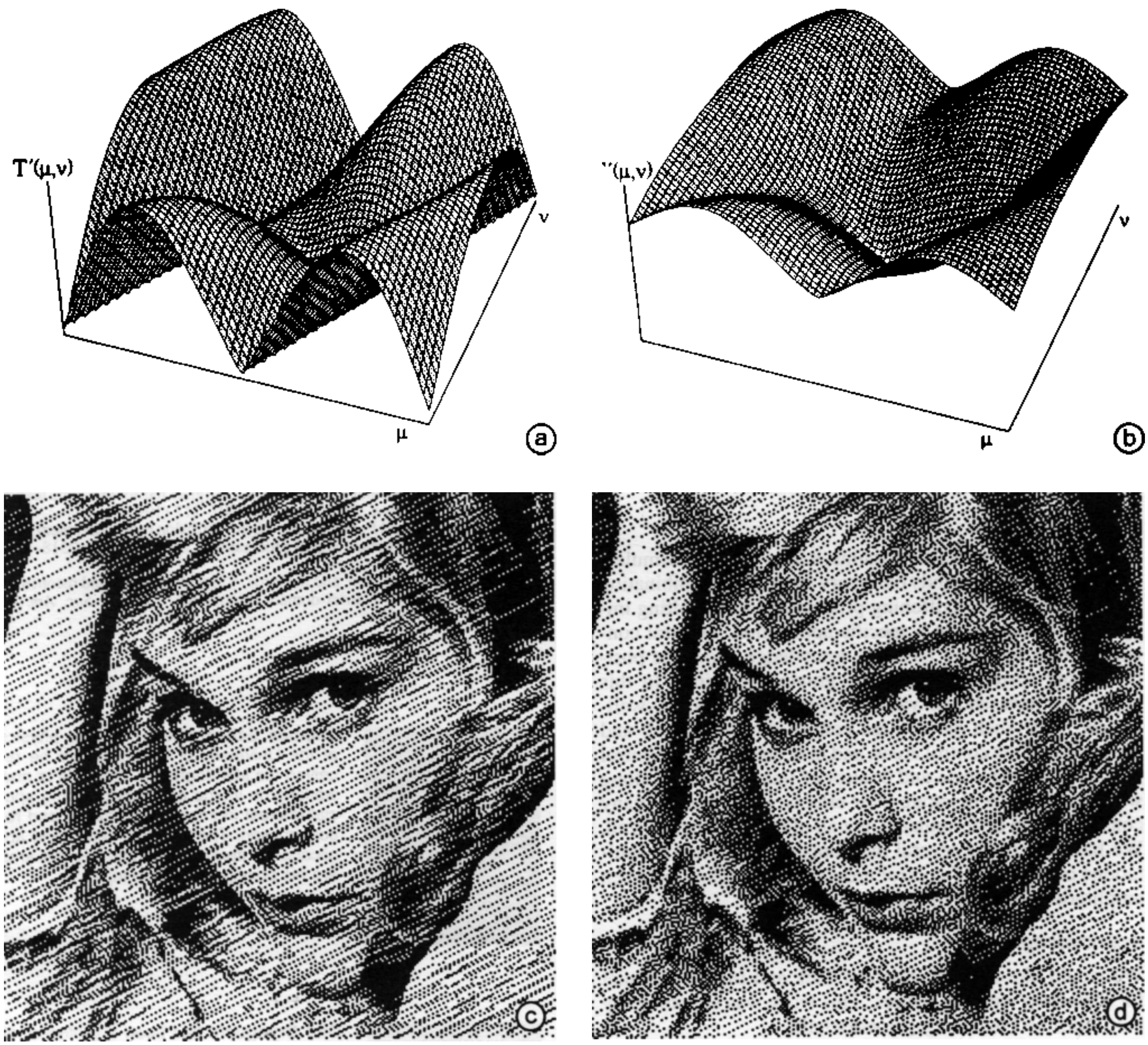

Figure 8. (a) and (b) Modified texture filters used for the synthesis of halftoned images and (c) and (d) corresponding binary images.

$$\omega_1 << \omega_3. \tag{20}$$

The smaller the control regions are, the more freedom exists and the easier it is to synthesize a binary image with the desired characteristics.

But even for $\omega_1 << \omega_3$, there is still a relation between the values in the control areas, provided that they are sufficiently large, because the coupling is of a local nature. Similar equations can be given inside a control region, with errors occurring mostly on the border of the area. The most important consequence is that amplitude and phase are interrelated.[13,18] Thus, control of the phase in Ω_2 implies a control of the amplitude, The amount of noise that can be introduced in the amplitude when controlling the phase is limited.

The fact that the resulting image is binary leads to an additional restriction, which can be formulated as a system of N^2 nonlinear equations in the same variables previously given. Again, the validity of these equations limits the possibilities to introduce noise and couples amplitude and phase in Ω_2, even if no oversampling is used.

If no sharply bounded control regions are used, but the noise spectrum is modulated according to a function as in Sec. 6, it is much more difficult to state the exact effect of the interrelations between the values in the spectrum on the realization of spectral constraints. It is clear that very strong demands are not compatible with the existence of a corresponding binary image. In the case of Sec. 6, this especially means that the integral over $1 - T'(\mu,\nu)$ has to be sufficiently small to ensure a proper convergence of the algorithm.

8 Conclusions

With the use of spectral constraints, it is possible to formulate a wide range of demands on binary images. In combination with the IFTA, the halftoning process and the resulting images can be adapted to a specific application. Spectral constraints may be either based on knowledge about the post-processing system or about the graytone original. In this paper, we have shown various types of constraints, well-known ones, such as lowpass control, phase control, and adaptation of the control areas, and new ones, such as control of the remaining noise and control of image textures, along with examples to illustrate their effects. Even though many constraints can be formulated, not all of them can be realized. We have discussed several mechanisms that result in limitations of the size of control areas and a coupling between amplitude and phase inside these regions.

Acknowledgments

We would like to thank Michael Tluk and Ingo Kummutat for their help with the figures. This work was supported by the Deutsche Forschungsgemeinschaft.

References

1. B. Bayer, "An optimum method for two-level rendition of continuous tone pictures," *Proc. IEEE* **1**, 26-11-26-15 (1973).
2. R. Floyd and L. Steinberg, "An adaptive algorithm for spatial grey-scale," *Proc. SID*. **17**(2), 75–77 (1976).
3. M. Broja, F. Wyrowski, and O. Bryngdahl, "Digital halftoning by iterative procedure," *Opt. Commun*. **69**, 205–210 (1989).
4. S. Kirkpatrick, C. Gelatt, Jr., and M. Vecchi, "Optimization by simulated annealing," *Science* **220**, 671–680 (1983).
5. J. Hopfield, "Neural networks and physical systems with emergent collective computational abilities," *Proc. Natl. Acad. Sci. USA* **79**, 2554–2558 (1982).
6. R. Mrusek, M. Broja, and O. Bryngdahl, "Halftoning by carrier and spectrum control," *Opt. Commun*. **75**, 375-380 (1990).
7. M. Broja and O. Bryngdahl, "Significance of spectral phase in synthesis of binarized images," *Opt. Commun.* **95**, 205–209 (1993).
8. T. Pappas, C.-K. Dong, and D. Neuhoff, "Measurement of printer parameters for model based halftoning," *J. Electron. Imag.* **2**(3), 193–194 (1993).
9. T. Scheermesser, M. Broja, and O. Bryngdahl, "Adaption of spectral constraints to electronically halftoned pictures," *J. Opt. Soc. Am*. **10**, 412–417 (1993).
10. R. Ulichney, "Dithering with blue noise," *Proc. IEEE* **76**, 56–79 (1988).
11. O. Bryngdahl, T. Scheermesser, and F. Wyrowski, "Digital halftoning: synthesis of binary images," in *Progress in Optics*, Vol. XXXIII, Elsevier Science B. V., Amsterdam (1994).
12. A. Oppenheim and J. Lim, "The importance of phase in signals," *Proc. IEEE* **69**, 529–541 (1981).
13. T. Scheermesser, M. Broja, and O. Blyngdahl, "Restrictions of spectral constraints in quantization of images," *Opt. Commun*. **99**, 264–273 (1993).
14. B. Julesz, "Visual pattern discrimination," *IRE Trans. Inf. Theory* 84–92 (1962).
15. S. Weissbach and O. Bryngdahl, "Control of halftone texture by error diffusion," *Opt. Commun*. **103**, 174–180 (1993).
16. T. Scheermesser and O. Bryngdahl, "Digital halftoning with texture control," *Electron. Publishing* **6**(3), 207–212 (1993).
17. S. Weissbach and F. Wyrowski, "Error diffusion procedure: theory and applications in optical signal processing," *Appl. Opt*. **31**, 2518–2534 (1992).
18. A. Oppenheim, J. Lim, and S. Curtis, "Signal synthesis and reconstruction from partial Fourier-domain information," *J. Opt. Soc. Am*. **73**, 1413–1420 (1983).

❋ Previously published in the *Journal of Electronic Imaging*, **4**(2) pp. 179–186, 1995.